

Switching of $K_{0.3}MoO_3$ at low temperatures. I. Response to the dc electric field

Atsutaka Maeda, Masaya Notomi,* and Kunimitsu Uchinokura

Department of Applied Physics, The University of Tokyo, 7-3-1 Hongo, Bunkyo-ku, Tokyo 113, Japan

(Received 23 February 1990)

Electric-field-dependent nonlinear conductivity and the current response in the time domain for dc electric fields were investigated in $K_{0.3}MoO_3$ at low temperatures, where a dramatic and sudden increase of the conductivity (we will refer to this increase as "switching") due to the collective contribution of the charge-density wave (CDW) was observed. The conductivity in the highly conducting state was found to increase with decreasing temperature, whereas the conductivity in the low-conducting state decreases with decreasing temperature. We interpret this phenomenon as a transition from the ordinary sliding state, which is already observed among various materials, to another sliding state with higher velocity, where the CDW can move without generating a backflow current of normal electrons. Around the threshold field for this switching, three kinds of current responses were observed in the time domain; these responses are likely to correspond to the three types of unit motions of the CDW. As a result of a detailed investigation of these responses, it is suggested that the current oscillation associated with the sliding motion of the CDW is usually generated in the bulk, but that the local mechanism for the generation of the oscillating current becomes dominant just around the switching threshold field. This implies that the amplitude mode should also be taken into account in order to obtain a correct description of the dynamics of the CDW.

I. INTRODUCTION

Quasi-one-dimensional materials have attracted much attention because they condense into various phases owing to inherent instability. In particular, charge-density waves (CDW's) attract a great deal of interest because they can be collective charge carriers.¹ Since the discovery of the collective motion of the CDW in $NbSe_3$ by Monceau *et al.*,² for more than a decade extensive studies have been made to clarify these highly peculiar phenomena.³

$K_{0.3}MoO_3$ is one of the quasi-one-dimensional materials⁴ that show the sliding conduction of the CDW's.⁵ The electric conductivity is highest in the direction where the MoO_6 octahedra form an infinite series.⁶ Owing to the strong one dimensionality of the electronic structure of $K_{0.3}MoO_3$,⁷ the destruction of the Fermi surface by the formation of the CDW is complete. Below the CDW transition temperature T_c ($=180$ K), in addition to the electric-field-dependent conductivity and the associated current oscillation,⁵ the low-frequency dielectric response is prominent in this material.⁸⁻¹² The excess conductivity decreases with decreasing temperature and approximately scales with the conductivity of the normal carriers that are thermally excited above the Peierls gap.¹³

Switching at the threshold field of 10–100 V/cm is observed below about 30 K.^{12,14,15} At this threshold the conductivity suddenly increases by several orders of magnitude. The direct observation of the inherent oscillation in this state¹⁶ clearly demonstrates that this phenomenon is also due to the sliding motion of the CDW. The switching phenomenon due to the participation of the CDW in the electrical conduction was already reported in $NbSe_3$ (Ref. 17) and TaS_3 (Ref. 18) and at much higher

temperatures in $K_{0.3}MoO_3$.^{5,19} However, the switching of $K_{0.3}MoO_3$ at low temperatures has the following characteristic aspect. In many cases of sliding, the motion of the CDW is associated with the screening effect of the normal electrons, which prevents the observation of the true features of the sliding CDW's.^{13,20,21} In the temperature region where switching becomes observable, however, almost no normal carriers are present. Thus, the bare response of the CDW is expected to be observed. However, the detailed features of this phenomenon have not been understood; it has been investigated both experimentally and theoretically by several groups.²²⁻³² We investigated in detail the response of $K_{0.3}MoO_3$ to dc and ac electric fields in the low-temperature highly conducting state attained by the switching. In this paper, the results of the field-dependent conductivity and the time-domain current response to the dc field is presented. The results of the response to the ac field will be presented separately.

A part of the present results were very briefly reported in Refs. 12, 16, 22, and 32.

II. EXPERIMENTS

Single crystals of $K_{0.3}MoO_3$ were prepared by the electrolytic reduction method described in Ref. 6. The resulting crystals were characterized both by powder and single-crystal x-ray-diffraction methods. The magnetic susceptibility was also measured in order to estimate the value of the local magnetic moment. As a result, it was found that the crystals usually have magnetic moments due to localized spins of the order of 1000 ppm on average. Samples appearing in this paper are described in Table I.

TABLE I. Samples appearing in this paper. "S" and "NS" in dc I - V characteristics denote switching samples and nonswitching ones, respectively, and "osc," "jump," and "RTO" denote the circuit-independent oscillation, discrete jumps, and circuit-sensitive relaxation-type oscillation, respectively. The symbol "II" in the last column represents figures appearing in the following paper.

Sample no.	dc I - V	Time-domain observation			ac conductivity	Figure no.
		osc	jump	RTO		
1	S				×	1,II1,II3
2	NS				×	1,II2,II4
3	S					2,3,4
4	S					5
5	NS					7
6	S					6
7	S	×	×	×		8,9,13
8	S		×	×		11
9	S		×	×		11
10	S	×	×	×		12

A conductivity measurement was performed by the two-probe method. Electrical contact was made by ultrasonically soldered indium. Electrical contact using several types of silver paste was also tried. The reproducibility with respect to heat cycles was not good when silver paste was used. We confirmed that the magnitude of the contact resistance was smaller than the resistance of the sample itself by comparing the resistance with that obtained by the four-probe method.

The dc electric conductivity was measured under both constant-voltage and constant-current conditions. For the constant-current measurement, a Keithley 220 current source was used, and the voltage drop across the sample was measured by a Keithley 617 electrometer. For the constant-voltage measurement, a Keithley 617 was used as a voltage source, and the voltage was applied to the circuit that included the sample and an Ohmic resistor in series with the sample. In this configuration, the Keithley 617 can provide a current of up to 2 mA. The resistance R_0 of the Ohmic resistor was selected to be much lower than that of the sample. The voltage drop across the Ohmic resistor was detected by a Yokokawa 2501A digital multimeter. In order to check the Joule-heating effect, a conductivity measurement with rectangular pulses was also performed. Rectangular pulses were applied by a Hewlett-Packard HP8116A pulse generator and amplified by an NF4005 amplifier, whose bandwidth is 1 MHz.

The time-domain measurement was performed mainly in the nearly constant-voltage condition. The current response (namely the voltage drop across R_0) was recorded by an Autronics S121 digital memory, whose capacity is 4 kilowords and the maximum sampling interval is 50 nsec.

III. EXPERIMENTAL RESULTS

A. The dc conductivity measurement

Figure 1 shows two different types of I - V characteristics of $K_{0.3}MoO_3$ obtained at low temperatures. In Fig. 1(a), discrete jumps were observed in both the increasing

fields and the decreasing fields. Within the resolution of 10 mV, both jumps were clearly observed. On the other hand, we sometimes obtain the sample which does not show the discrete jump or the hysteresis as is shown in Fig. 1(b) (we will call it the "nonswitching" sample). We sometimes obtain nonswitching samples after several heat or field cycles on the switching sample, whereas we never got the switching sample from the nonswitching sample. The origin of the different I - V characteristics will be discussed in Sec. IV D. It should be noted that for both types of samples, the conductivity depends on the electric field even below the sudden increase of conductivity. We could not observe any hysteresis in this field region.

In most of the samples we investigated, the observation of the high-field conductivity in the highly conducting state was impossible, owing to the Joule-heating effect even in the pulsed measurements. However, there were a

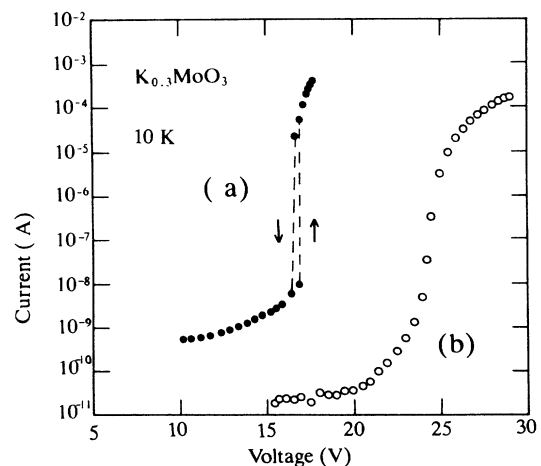


FIG. 1. The I - V characteristics of (a) a switching sample (no. 1) and (b) that of a nonswitching sample (no. 2) of $K_{0.3}MoO_3$. Dashed lines are a guide for the eye.

few cases where we could perform the detailed investigation of the conductivity in the highly conducting state at various temperatures. Figure 2 shows the voltage dependence of the conductivity of a switching sample (no. 3) at various temperatures. A large hysteresis is observed at the switching-threshold field. The width of the hysteresis increases with decreasing temperature. Figure 3 shows the temperature dependence of the threshold voltage of the switching V_T in this sample. Although the temperature dependence of V_T is weaker than that in high-temperature region,¹² V_T takes a minimum value at around 12 K. The conductivity in the highly conducting state σ_{on} increases with decreasing temperature, whereas the conductivity in the low-conducting state σ_{off} decreases with decreasing temperature. In order to compare the temperature dependence of σ_{on} and that of σ_{off} much more definitely, the conductance at 45 and 57 V were drawn as a function of temperature in Fig. 4. In Fig. 4, we regard the value of the conductance at 45 and 57 V as σ_{off} and σ_{on} , respectively. In Fig. 4, σ_{off} decreases with decreasing temperature, and behaves as though it is thermally activated with an activation energy of 20 mV. On the other hand, σ_{on} increases with decreasing temperature. Thus, the increase in conductivity by the switching decreases with increasing temperature. The observed temperature dependence of σ_{on} is highly unusual if we consider the scaling relation between the conductivity due to the uncondensed carrier σ_0 and that due to the CDW (σ_{CDW}), which has been reported to hold in various materials including this material in the high-temperature region.^{13,20,21} Even in samples whose σ_{on} was investigated in detail, very slight Joule-heating may be unavoidable in the highly conducting state even for the pulse measurement. Thus, the true $\sigma_{on}(T)$ may be slightly different from the observed $\sigma_{on}(T)$. However, the tendency for σ_{on} to decrease with increasing temperature is probably true. If we assume that σ_{on} increases with in-

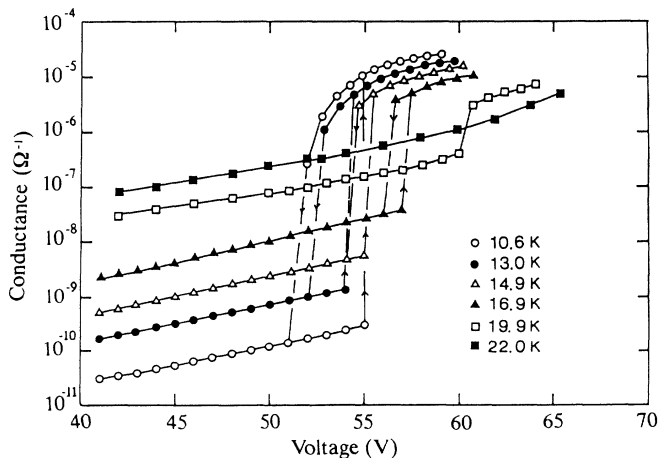


FIG. 2. The conductance of a switching sample (no. 3) as a function of applied voltages at various temperatures. Solid curves are a guide for the eye.

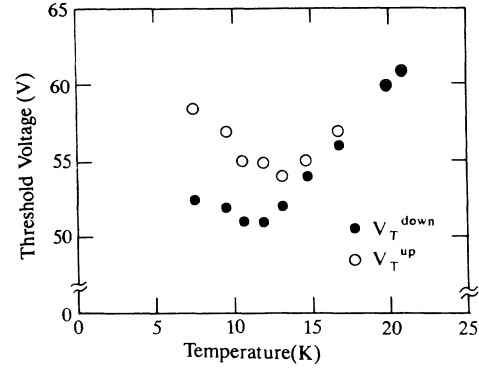


FIG. 3. The temperature dependence of the threshold field for switching of sample no. 3.

creasing temperature, the Joule heat produced under the constant-voltage condition increases with increasing temperature. Therefore, $d\sigma_{on}/dT$ would stay positive even when Joule heat is produced, irrespective of the temperature dependence of the heat capacity. In this sense, we think the Joule-heating effect did not play an essential role in the conclusion we reached here.

As shown in Fig. 2, the conductivity in the low-conducting state σ_{off} is also dependent on the electric field, and behaves as

$$\sigma_{off} = \sigma_1 \exp[-(\Delta_0 - aE)/k_B T] \quad (3.1)$$

as a function of the electric field E and temperature T above 13 K, where σ_1 , Δ_0 , and a are constants.

Figure 5 shows the I - V characteristics of sample no. 4 at 29.7 K. In Fig. 5, I is linear in V around zero field, and the switching occurs at around 15 V. Thus, we think that the nonlinear conduction below the switching-threshold

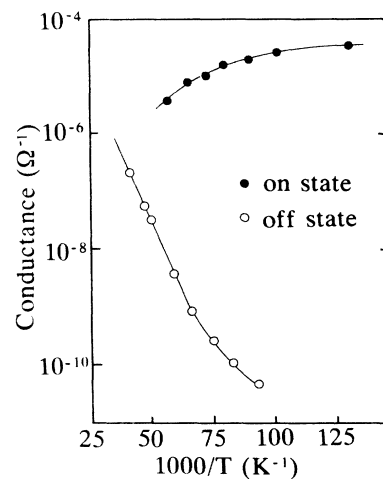


FIG. 4. The temperature dependence of the conductance in the highly conducting state σ_{on} ($V = 57$ V) and that in the low-conducting state σ_{off} ($V = 45$ V) obtained in sample no. 3.

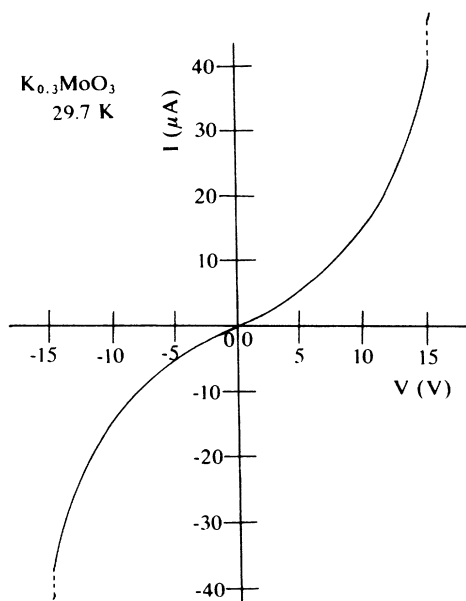


FIG. 5. The I - V characteristics of sample no. 4 measured at 29.7 K.

field and the switching itself are a separate phenomena. Hereafter, we call the former threshold and the switching one E_T and E'_T , respectively.

It should be also noted that in Fig. 2 the increase of the conductivity at E'_T seems to become zero continuously with increasing temperature at around 22 K.

Figure 6 shows the comparison of the I - V characteristics observed in the constant-current condition and the constant-voltage condition. In the constant-voltage condition, clear jumps were observed both in decreasing and increasing fields. On the other hand, in the constant-

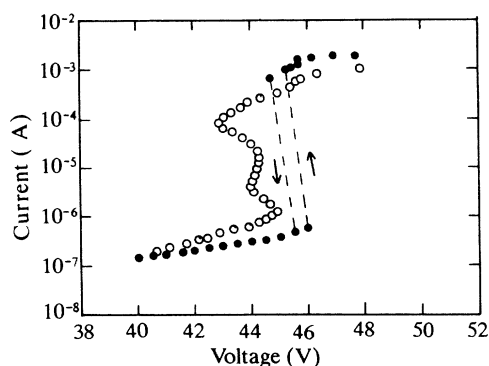


FIG. 6. I - V characteristics of a switching sample (no. 6) obtained both in constant-current condition (open circles) and in constant-voltage condition (solid circles). For the data obtained in the constant-voltage conditions, hysteresis and observed for the voltage sweep. Dashed lines are a guide for the eye. On the other hand, in constant-current condition, no hysteresis is observed for current sweep.

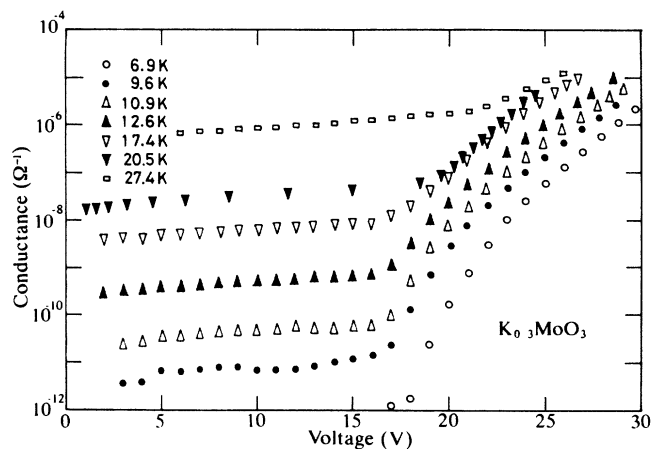


FIG. 7. The conductivity of a nonswitching sample (no. 5) as a function of voltage at various temperatures.

current condition, the S-like I - V characteristics with negative differential resistance were observed. The S-like I - V characteristics were also observed by Martin *et al.*²⁷

Figure 7 shows the electric-field dependence of the nonlinear conductivity of a nonswitching sample (no. 5) at various temperatures. The conductivity at high fields decreases with decreasing temperature, which is in contrast to the temperature dependence of σ_{on} in switching samples.

B. The current response in the time domain

Figure 8 shows the current responses observed in a switching sample at various applied voltages. The I - V characteristics of this sample are shown in the inset of Fig. 9. When the load line of the circuit has no crossing point, the current response is the relaxation-type oscillation shown in Figs. 8(a) and 8(b). With increasing applied voltages, different types of the oscillation began to be observed, as shown in Figs. 8(c)–8(h). With further increasing applied voltages, the oscillation could not be found in the time domain [Fig. 8(i)]. However, the spectral analysis in the frequency domain clearly shows the existence of the well-defined peak and its harmonics. Previously, we showed¹⁶ that the frequency of the latter type of the oscillation does not depend on the external passive element, and that this oscillation is the inherent oscillation associated with the sliding motion of the CDW.^{33,34} Figure 9 shows the frequency of the oscillation as a function of the average current, together with that of the circuit-dependent relaxation-type oscillation (RTO).³⁵ The frequencies of both types of oscillation are roughly proportional to the average current. It should be noted that two branches were observed even for the circuit-independent oscillation.

Figure 10 shows the period of the RTO as a function of the total capacitance C_{tot} , which is the sum of the capacitance C_0 existing without any external capacitance and

the externally attached capacitance C_{ext} parallel to the sample (see Fig. 11 for the circuit). The value of the capacitance C_0 was estimated assuming that the period increases linearly with increasing C_{ext} for small C_{ext} , which is shown in the inset of Fig. 10. C_0 was found to be 90 pF, which is of the same order of magnitude as the stray capacitance of the circuit. Furthermore, for comparison, the period of the RTO observed in a neon tube instead of the sample is also shown in Fig. 10. The period P increases with increasing C_{tot} as $P \propto C_{\text{tot}}^{0.8}$ for C_{tot} larger than about 4×10^{-10} F.

The current response just above E_T' was sometimes stepwise as shown in Fig. 12. The histogram of the magnitude of the current jumps clearly shows that the jump magnitude was always the integer multiples of a unit value.²² This quantization was also observed in TaS₃.³⁶ With increasing applied voltages, the stepwise response changes into the oscillation gradually.²²

Near E_T' , the current response was also intermittent when observed with a longer time scale,³⁵ which is the origin of the broadband noise with the Lorentz spectrum in the frequency domain.³⁵ The temperature dependence of the characteristic time of the intermittency was found

to be of the Arrhenius type.²² Thus, it is likely that the intermittency is caused by the thermal fluctuation, and not due to the chaotic nature of the nonlinear system. A detailed discussion will be given in Sec. IV F.

IV. DISCUSSION

A. Is the switching due to the sliding of the CDW?

The observation of the inherent current oscillation in the time domain and the frequency domain definitely shows that the conductivity increase at E_T' is due to the sliding motion of the CDW. The current oscillation was often observed in the time domain at the beginning of the response to the rectangular pulsed voltage.³⁷ In that case, the amplitude of the oscillation decays and vanishes after several cycles. This has been interpreted to be due to the degradation of the phase coherence of the CDW as the time passes. Thus, the time-domain observation of the current oscillation for the stationary dc voltage is difficult except for a few cases.³⁸ Thus, the present result clearly means that in the highly conducting state the phase coherence of the sliding CDW is well developed.

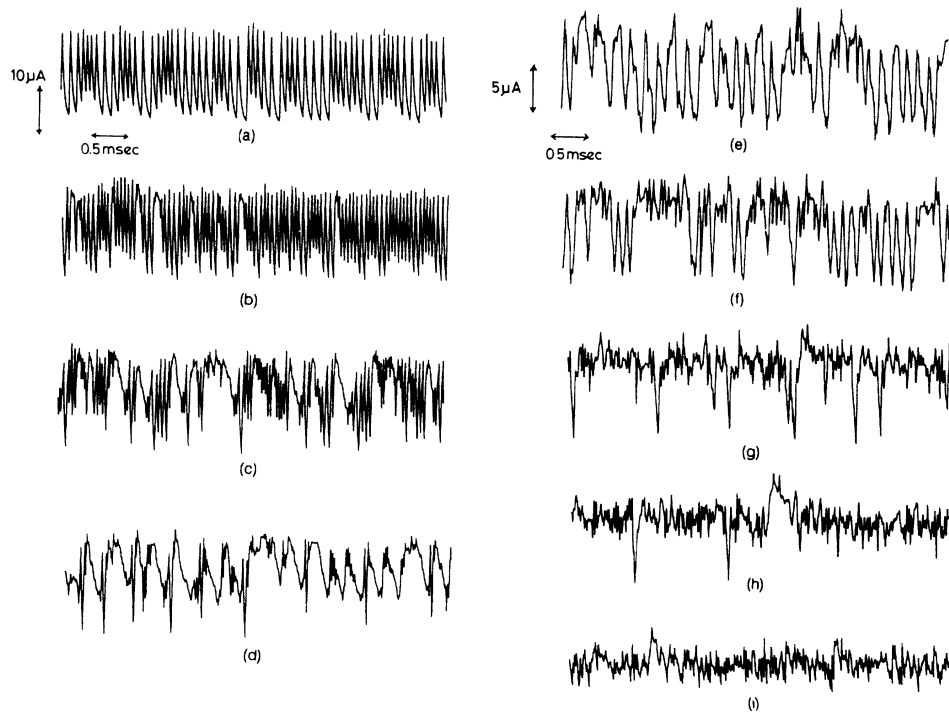


FIG. 8. The current response observed in a switching sample (no. 7) at various averaged currents at 10.7 K. (a) 10 μA , (b) 16 μA , (c) 20 μA , (d) 25 μA , (e) 40 μA , (f) 50 μA , (g) 78 μA , (h) 80 μA , and (i) 102 μA .

B. The origin of the energy dissipation of the CDW in the highly conducting state above E_T'

As was already shown in Fig. 4, in switching samples, σ_{on} did not scale with σ_{off} , in contrast to the result obtained at a higher-temperature region in the same material.¹³ The scaling relation between σ_0 and σ_{CDW} is also well established in other materials.^{20,21} This is interpreted as a result of the screening of the deformation of the sliding CDW by normal carriers.³⁹

Experimentally, it is clear that the CDW suffers finite damping when it moves, which prevents the occurrence of the so-called Fröhlich superconductivity.¹ The origin of the damping was considered theoretically by several authors. Boriak and Overhauser⁴⁰ proposed that the finite damping is possible by the drag of normal carriers interacting with impurities. Takada *et al.*⁴¹ proposed the damping through the interaction between the thermally activated phason modes, and calculated the temperature dependence of the relaxation time, which behaves as

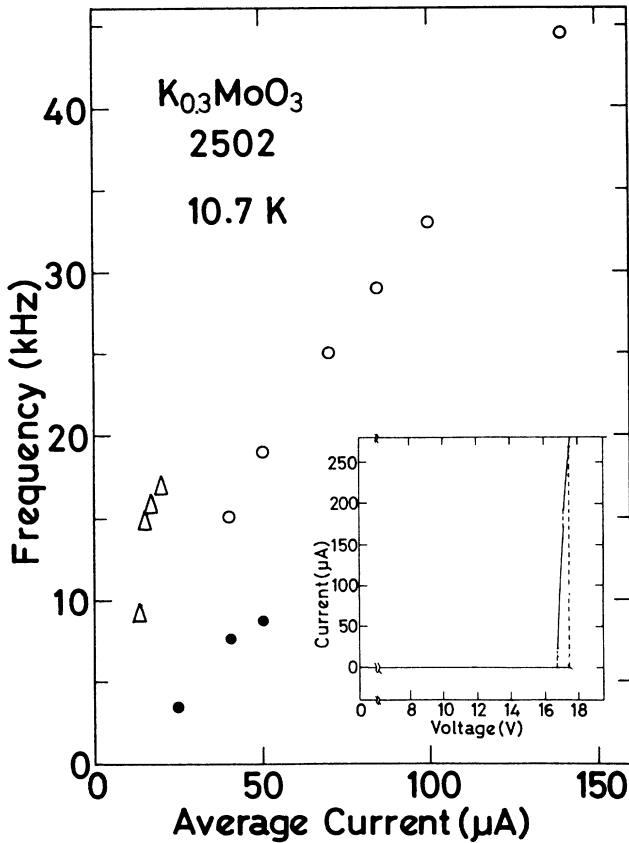


FIG. 9. The frequency of the current oscillation as a function of the average current for sample no. 7. Circles and triangles are for circuit-independent oscillation and for circuit-dependent RTO, respectively. Open and solid symbols represent that each belongs to the different branches with different current to frequency ratios. The inset shows the I - V characteristics of the same sample.

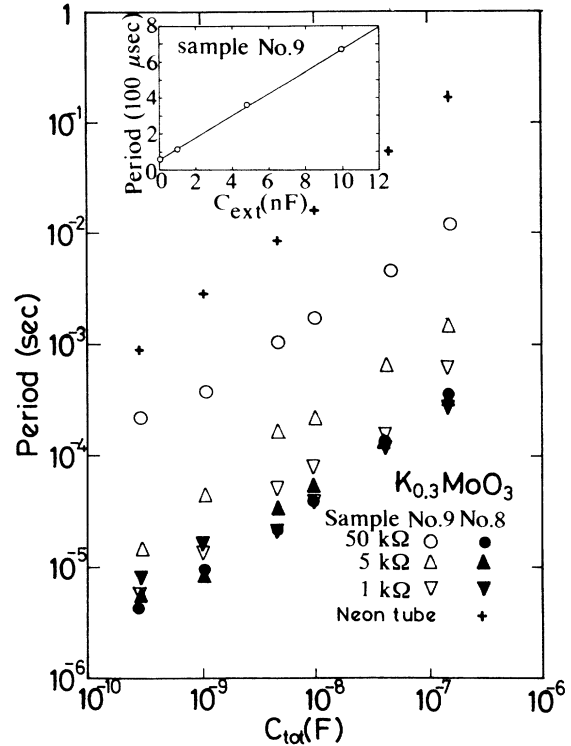


FIG. 10. The period of the RTO for various series resistance R_0 as a function of the total capacitance C_{tot} in sample no. 8 (solid symbols) and in sample no. 9 (open symbols). As a reference, the period of the RTO observed in the circuit where the sample was replaced by a neon gas tube was also shown. The inset shows the period of the RTO as a function of the externally attached capacitance C_{ext} .

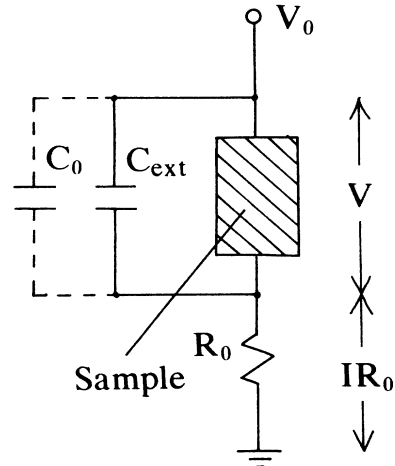


FIG. 11. Schematic drawings of the circuit used in the experiments discussed in this paper.

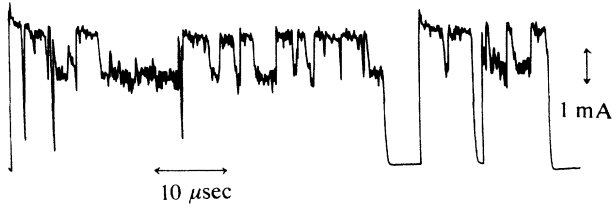


FIG. 12. An example of the stepwise current response observed in a switching sample (no. 12) for a pulsed dc voltage of 43.5 V. Repetition rate and the duration of the pulse are 1.4 kHz and 75 μ sec, respectively.

$$\tau \propto T^{-2} \text{ for high temperatures,} \quad (4.1)$$

$$\tau \propto T^{-5} \text{ for low temperatures.} \quad (4.2)$$

They also calculated the contribution of the amplitude mode to the damping, which was found to be much smaller than that by phason-phason interaction.

In almost all of the experiment, however, the damping of the CDW is dominated by the screening of the CDW deformation by the normal carriers rather than by the microscopic mechanisms introduced just above.^{13,20,21} In the low-temperature region of $\text{K}_{0.3}\text{MoO}_3$, the same mechanism is valid at least in the weak-field region. However, in the highly conducting state in the same temperature region, the breakdown of the scaling relation between σ_{on} and σ_{off} clearly demonstrates that the damping in the highly conducting state is irrelevant to the screening by the normal carriers. Kim *et al.*⁴² proposed that a finite gap appears in the phason spectrum under the presence of the long-range Coulomb interaction, which prevents the deformation of the CDW condensates. However, the ac conductivity measurement under the dc bias larger than E'_T (Ref. 32) suggests that the coherent deformation (phason excitation) is still present even in the sliding state. Therefore, the weakly temperature-dependent σ_{on} suggests that the phason-phason mechanism or phonon-phason mechanism⁴¹ is partly responsible for the damping. In many samples, we could not observe finite σ_{on} partly because of the destruction of the samples and the contacts due to the heating effect and partly because of the true high value of σ_{on} . Thus, it seems that σ_{on} strongly depends on samples. When the “dirty” samples were obtained “fortunately,” the experimental observation of σ_{on} may be possible. Therefore, the interaction between the CDW and the impurities may also be responsible for the mechanism of the damping in the highly conducting state.

Here we should mention that the different I - V characteristics were reported by Mihaly *et al.*²⁵ In their report, the S-like characteristics were not observed, and σ_{on} in their sample was reported to be larger than $10^4 \Omega^{-1} \text{cm}^{-1}$, whereas ours are $10^{-2} \Omega^{-1} \text{cm}^{-1}$ at best. Although the difference of the magnitude of σ_{on} can be explained by the above-mentioned picture, the difference on the existence of the S-like characteristics are not known.

C. The nonlinear conduction below the switching threshold field

As was shown in Fig. 2, the conductivity below E'_T is also nonlinear. This nonlinearity seems to be connected to the ordinary nonlinear conduction at higher temperatures. As was mentioned in Sec. III A, this nonlinear conduction was found to be a separate phenomenon from the switching. Thus, irrespective of whether the switching takes place in the high-field region at low temperatures or not, the nonlinearity of the I - V characteristics in the lower-field region exist. Thus, it is likely that the nonlinear conduction below E'_T at low temperatures is the same kind of phenomenon as that at higher temperatures, that is, the nonlinear conduction due to the sliding motion of the CDW. Thus, the switching or strong increase of conductivity at E'_T should be regarded as the transition from a sliding state to another sliding state, which is in agreement with Refs. 26, 27, and 29, but in disagreement with Ref. 42. The difference of the sliding motion below and above E'_T will be discussed in the next section.

D. The origin of the switching at low temperatures

The switching phenomenon associated with the nonlinear conduction of the CDW is often observed in this material and in other materials.¹⁷⁻¹⁹ In NbSe_3 , the effect of the amplitude mode is proposed as the origin of the switching.⁴³ Theoretically, several models were also proposed, including the effect of the viscous interaction between domains,⁴⁴ and the phase-slip process among strong impurities.⁴⁵ However, all of these models were based on the assumption that the CDW is pinned below the threshold field, which is in contrast to our experiment. Thus, these models cannot be compared with the present experimental results directly.

Even if we assume that these models are applicable to the present problem, it should be mentioned again that the frequency dependence of the ac conductivity under the dc bias above E'_T can be well explained³² by the Fukuyama-Lee-Rice (FLR) model,^{46,47} in which only the dynamics of the phase was included. Thus, it is likely that the amplitude mode plays no crucial role in the highly conducting state above E'_T . Microscopic theoretical calculation⁴¹ also showed that the effect of the amplitude mode on the damping of the CDW is small. Thus, it is unlikely that the amplitude mode introduces a qualitative change in the damping of the sliding CDW. The above models only explain the appearance of the discrete jumps in the I - V characteristics, but do not explain the qualitative difference appearing in the temperature dependence of $\sigma(E)$ between the two states described in Sec. III A. Thus, in order to explain the switching phenomena in $\text{K}_{0.3}\text{MoO}_3$ at low temperatures, a quite different approach seems necessary.

Recently, Littlewood²⁶ proposed a model which treats explicitly the low-temperature switching of $\text{K}_{0.3}\text{MoO}_3$. In this model, the origin of the switching is closely related to the effect of the screening of the deformation of the CDW by the normal carriers, and the switching occurs

only in semiconducting materials like TaS_3 , $K_{0.3}MoO_3$, and $(TaSe_4)_2I$. In general, random deformations are induced when the CDW moves, because of the existence of pinning centers. According to the continuity equation, the backflow current of the normal carriers is generated in order to screen the polarization induced by the CDW, which produces the energy dissipation. Thus, the lifetime of the sliding CDW is restricted by the conductivity σ_0 of the normal carriers. In the semiconducting materials, σ_0 is due to the thermally activated normal carriers. Thus, the lifetime of the damping of the CDW, τ_{CDW} , becomes long with decreasing temperature as

$$\tau_{CDW} \propto \exp(\Delta/k_B T), \quad (4.3)$$

where Δ is a constant. For instance in $K_{0.3}MoO_3$, at 25 K, τ_{CDW} reaches 22 min.⁹ Thus, in this temperature region, the screening of the deformation is almost impossible. In this situation, when the CDW is accelerated, the damping force acting on the moving CDW becomes closer to that without the screening. The result of numerical calculation of the I - V characteristics based on this picture shows that the S-like bistability appears only at low temperatures. This means that the switching I - V characteristics are obtained in the constant-voltage configuration. In this model, the switching occurs only after the first depinning of the CDW. Thus, the I - V characteristics are nonlinear even below E'_T . This is consistent with our consideration that the nonlinear conduction below E'_T is also due to the sliding motion of the CDW. The appearance of the S-like I - V characteristics under the constant-current configuration in our experiment (Fig. 6) is in agreement with this model, but is in disagreement with other models introduced previously.⁴³⁻⁴⁵

Another important experimental result is the existence of the finite time delay in the time-domain current response.¹² In this model, a finite time is required until the velocity of the CDW reaches the critical value for the switching to occur. This just corresponds to the finite delay time observed in the time-domain current response. The temperature dependence and the electric-field dependence of the time delay is also consistent with this model. Thus, the switching in $K_{0.3}MoO_3$ at low temperatures is considered to be due to the change in the damping force acting on the CDW, as was proposed by Littlewood.²⁶

Next, we should discuss the origin of the difference between the nonswitching and the switching I - V characteristics shown in Fig. 1. The most trivial reason for the absence of the discontinuous jump at E'_T is the inhomogeneous current distribution in such samples. However, the inherent oscillating current was often observed more definitely in nonswitching samples than in switching samples.⁴⁸ Moreover, there is definite difference in the temperature dependence of the conductivity in the highly conductive state in high-field region, as was shown in Figs. 2 and 7. This difference cannot be understood only in terms of the degree of macroscopic inhomogeneity of the current distribution in samples. Thus, we think that other intrinsic factors are correlated with whether the I - V characteristics have a discontinuity or not. Here, we

should note that the continuous I - V characteristics appear also in Littlewood's model introduced just above. Within the framework of this model, the continuous I - V characteristics were obtained for low-dimensional (less than two) bulk systems.

Distribution of the time constant for the screening of the CDW deformation due to the distribution of the pinning potential may also lead to the continuous I - V characteristics. The increasing conductivity with increasing temperature even in the high-field region in nonswitching samples will be explained also in terms of the distribution of the characteristics time for screening.

E. The unit motion of the CDW and the effect of the amplitude mode

1. The stepwise current response

The experimental results performed in the time domain showed that the CDW has various responses to the applied field, reflecting the absence of the normal carriers.

The current response was sometimes stepwise and quantized. This kind of response can be interpreted in terms of the creation and annihilation of vortices of the CDW phase.^{36,49} According to this model, the current response is composed of a series of random jumps near the threshold field, where the distance between vortices is long. With increasing field, the distance between vortices becomes shorter and vortices begin to move coherently. Thus, the current response is expected to become the regular oscillation. In our experiment, the crossover from the stepwise response to the relaxation-type oscillation was observed.²² This behavior seems to coincide with that expected by the vortex model. The quantitative estimation also agrees with this model well.²² Thus, the stepwise response in $K_{0.3}MoO_3$ can be well explained by the creation and annihilation of the phase vortices. This simultaneously means that the dynamics of the amplitude mode should be taken into account in the more detailed description of the sliding motion of the CDW.

2. The relaxation-type oscillation (RTO)

In the situation where the I - V characteristics of the sample in the constant-voltage configuration do not have any crossing point with the load line of the circuit, the RTO was observed, as was shown in Fig. 8. The period of the oscillation depends on the external capacitance C_{ext} . This type of oscillation is also possible without the inherent periodicity. A typical example of this type of oscillation is that of a neon gas tube. The current can oscillate by the repetition of charge and discharge of the parallel capacitor C_{ext} . Thus the period of the oscillation, and also the charge contained in one period is proportional to C_{ext} , and the net current flows in the on state. More generally, these behaviors can be described by the van der Pol equation,

$$d^2x/dt^2 + \mu(x^2 - 1) dx/dt + x = 0, \quad (4.4)$$

where x is the time derivative of the output current, t is time, and μ is a positive parameter.

The RTO in $K_{0.3}MoO_3$ surely possesses the above characteristics. However, it is clear that, at least, the on state (highly conducting state) is due to the sliding motion of the CDW's. Therefore, even if the RTO observed in $K_{0.3}MoO_3$ is easily influenced by the external circuit, the charge contained in each period is carried by the CDW. Thus, it can be concluded that at least the current corresponding to the one-wavelength motion of the CDW is involved under each oscillation. Thus, in the limit $C_{ext} \rightarrow 0$, it is likely that each RTO corresponds to the unit motion of the CDW. In this viewpoint, the increase of the charge involved in each oscillation with increasing C_{ext} can be interpreted in the following two ways. One possibility is that the distance over which the CDW moves under each oscillation increases with increasing C_{ext} . An alternative possibility is that the cross section through which the coherent motion of the CDW occurs increases with increasing C_{ext} . In the former case, some structure may appear in the time-domain current response corresponding to each one wavelength of the motion, which is not observed in our experiment. On the other hand, in Fig. 9, even for the circuit-independent oscillation, two branches with different I_{CDW}/f ratio (I_{CDW} is the current carried by the CDW, and f is the frequency of the oscillating current) were observed, which means that the coherent cross section in the sliding state can easily be changed. Thus, the latter possibility seems more likely. From this point of view, the saturation of the charge involved in each oscillation is expected to be observed with further increasing C_{ext} . We have not succeeded in observing such saturation, because the switching vanishes with further increasing C_{ext} . Thus, the external circuit was found to affect the I - V characteristics. Figure 13 shows the current response at the same bias voltage with different C_{ext} . Without any externally attached capacitor, the inherent oscillation was observed in the frequency domain at around 40 kHz. On the other hand, with a capacitor of 0.047 μ F, the relaxation-type oscillation appeared. Thus, this result also showed that the C_{ext} surely affects the I - V characteristics.

At present, the origin of this change is puzzling. In the following, however, we show a simple numerical simula-

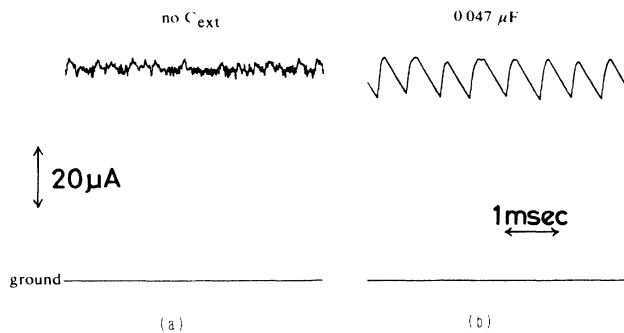


FIG. 13. The current responses of a switching sample (no. 7) at the same dc bias voltage with different C_{ext} .

tion which treats the motion of the CDW and the external circuit simultaneously. This may give some clue for the understanding of this phenomenon.

The equivalent circuit of the experiment shown in Fig. 11 is represented as

$$I = (V/R_0) - [1 + (R_0/R_{off})](V/R_0) - C_{tot} dV/dt \quad (R_{off} > R_0), \quad (4.5)$$

$$I = Sn_c e dx/dt, \quad (4.6)$$

where V_0 is the applied voltage on the sample plus the Ohmic resistance R_0 , V , and I are the voltage drop across the sample and the current through the sample, respectively, R_{off} is the resistance of the sample in the low-conducting state, C_{tot} is the capacitance parallel to the sample, t is time, n_c is the carrier density condensed into the CDW, e is the electronic charge, x is the coordinate of the CDW, and S is the cross section of the sample. For simplicity, the I - V characteristics below the switching-threshold field are assumed to be linear. Considering the highly coherent nature in the highly conducting state, the motion of the CDW is assumed to be described by the simplest version of the classical model, namely the single-particle "washboard" model:⁵⁰

$$d^2x/dt^2 + \gamma dx/dt + (1/Q)\omega_0^2 \sin Qx = eE/m^*, \quad (4.7)$$

where m^* and Q are the effective mass and the wave vector of the CDW, respectively, γ is the damping of the CDW, ω_0 is the pinning frequency, and E is the applied electric field, which is connected to the voltage V as $V = El$, where l is the length of the sample. As was already discussed in Sec. IV D, we think that the switching is a transition from a sliding state to another sliding state. On the other hand, this model clearly regards that the CDW is pinned below E'_T . However, as will be seen below, the application of this model does not affect the conclusion of this section. Below, the term with second derivative is neglected because the CDW motion in this material is overdamped.³⁰ Substituting Eqs. (4.6) and (4.7) into Eq. (4.5), and by the moderate scale transformation, the following equations were obtained:

$$d^2\theta/d\tau''^2 + B(\theta)d\theta/d\tau'' + \sin\theta = \epsilon_0, \quad (4.8)$$

$$B(\theta) = \omega_0(t_D t_S)^{1/2} (K + \cos\theta), \quad (4.9)$$

$$K = (\omega_0 t_S)^{-1} G + H, \quad (4.10)$$

$$H = R_0 S n_c e / l E_T t_S Q, \quad (4.11)$$

$$t_D = 1/\gamma, \quad (4.12)$$

$$t_S = R_0 C_{tot}, \quad (4.13)$$

$$\tau'' = \omega_0 (t_S / t_D)^{1/2} t, \quad (4.14)$$

$$\epsilon_0 = V_0 / l E_T, \quad (4.15)$$

where θ is the phase of the CDW. In Eq. (4.8), if we take $E'_T = 10$ V/cm, $S = 10^{-2}$ cm², $l = 10^{-1}$ cm, $n_c = 10^{21}$ cm⁻³, $R_0 = 5$ k Ω , $C_{tot} = 400$ pF, $\omega_0 = 10^{12}$ Hz,³⁰ $1/\tau = 50$ GHz,³⁰ then $\alpha = 10^{-4}$ and $G = 5$, and $H = 0.1$. Then, we got $K = 0.1$. Thus, the sign of "the damping term" $B(\theta)$

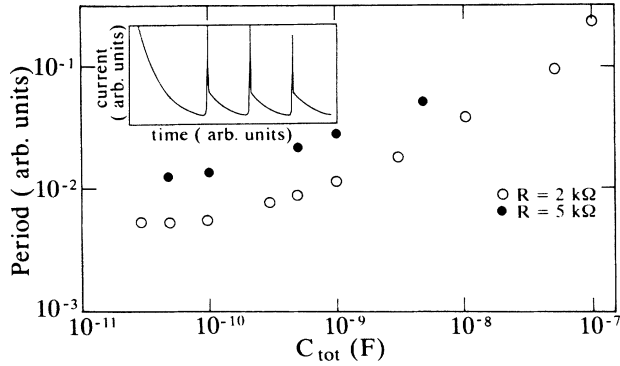


FIG. 14. The dependence of the period of the oscillation obtained by the numerical calculation of Eq. (4.7) on the capacitance C_{tot} for $\epsilon_0 = 1.1$, $\omega_0 = 10^{12}$ Hz, and $t_D = 10^{-11}$ sec. The open and solid circles are for $R_0 = 2$ and 5 k Ω , respectively. The inset shows an example of the time dependence of the current ($C_{tot} = 10^{-9}$ F and $R_0 = 2$ k Ω).

changes when the time proceeds in one period. This is analogous to the van der Pol equation [Eq. (4.4)]. Thus, the RTO accompanying the sliding motion of the CDW is expected. In fact, numerical calculation shows the current response as shown in the inset of Fig. 14. Figure 14 shows the dependence of the period of the oscillation on C_{ext} . Because of the existence of the inherent periodicity, the period is not simply proportional to C_{tot} . Thus, the experimental results in Fig. 10 probably correspond to the region of intermediate C_{tot} . This analysis may also explain the slight difference in the dependence of the period of the oscillation on C_{tot} between $K_{0.3}MoO_3$ and the neon gas tube, shown in Fig. 10.

Equation (4.8) with the parameters used above does not show the I - V characteristics with discontinuous jumps. Thus, the analysis presented here is far from the real situation. However, what we stress in this analysis is that for the highly coherent motion of the CDW, the external circuit strongly affects the current response of the CDW. In particular, increasing the C_{ext} leads to the appearance of the RTO and an increasing coefficient of $B(\theta)$. Thus, CDW suffers large “damping” (negative or positive) for large C_{ext} . This may make a larger cross section to participate in the sliding motion. This will explain the observed increase of the charge contained in each oscillation.

3. The three types of the unit motion of the CDW and their interrelation

From the above argument, it can be concluded that at least three types of unit motions exist in the sliding of the CDW. That is (1) the current oscillation independent of the external circuit, (2) the RTO which is strongly affected by the external circuit, and (3) the quantized stepwise response.

The quantized response and the RTO were only observed in the voltage region where the I - V characteristics

show the discrete jumps. The quantized response was well explained by the phase-vortex model.⁴⁹ Thus it can be said that the phenomena in which the amplitude mode plays an important role can be observed in the electric-field region where the I - V characteristics are unstable. Here, it should be noted that there is another possibility in the destruction of the CDW amplitude other than the creation and annihilation of phase vortices. Gor’kov *et al.*⁵¹ proposed that in some samples the phase-slip process is more favorable than the creation-annihilation of vortices. In this process, the amplitude of the CDW is completely destroyed on a whole plane normal to the current direction. Our experimental result is that with increasing applied field, the stepwise response changes into the RTO. Thus, if the stepwise response is understood in terms of the vortex model, the RTO may correspond to the phase-slip process. With increasing applied voltage, the number of the vortices increases and the distance between them becomes shorter. Thus, in order to carry much more current, the phase-slip process becomes naturally preferable.

We speculate, however, that in usual cases the pinning is likely dominated by that in the bulk. The current oscillation is generated as the bulk effect, as was also shown by the numerical simulation based on the FLR model.^{52,53} At the same time, the vortex generation or the phase-slip process may occur at the interfaces. However, these processes are probably not dominant. They become dominant only in the field region where the I - V characteristic shows a discrete jump. In this region, the CDW can move fast in the bulk, but cannot move at the interface (electrical contacts, etc.) due to the pinning there. Thus, the effect of the amplitude mode is expected to become dominant.

F. Intermittency

The current response to the dc field is often intermittent near E_T' . In the presence of the bistability, there are two possibilities for the origin of the intermittency. One is the transition between the two states due to the fluctuation of thermal⁵⁴ or quantum origins.⁵⁵ In fact, it was observed in the resistivity-shunted Josephson junction.^{56–58} The other is the chaotic response without any stochastic fluctuations, which is characteristic of the nonlinear systems.⁵⁹ Previously, based on the phenomenological two-valued process model, we showed that the intermittency is due to the fluctuations which have a thermal origin.²²

Grassberger and Procaccia⁶⁰ proposed a method which can determine whether the observed intermittency has the thermal origin or the chaotic origin by estimating the dimension of the attractor, using the time series data obtained by the experiment.^{60,61} By this method, it was also shown that the intermittency observed in $K_{0.3}MoO_3$ can be interpreted as the transition between two metastable states due to the thermal fluctuation.⁴⁸

To be more quantitative, the average lifetime in the low conducting state τ_{off} is represented as follows:

$$\tau_{off} = \tau_{off}(E) \exp[U(E)/k_B T], \quad (4.16)$$

$$U(E) = U_0(1-x)^{3/2}, \quad (4.17)$$

$$\tau_{\text{off}}(E) = \omega_p^{-1}(1-x^2)^{-1/4}, \quad (4.18)$$

where $x = E/E_T'$ and $U_0 = eE_T'\lambda_{\text{CDW}}$, which is the effective barrier from the low-conducting state of the highly conducting state, λ_{CDW} is the wavelength of the CDW, and ω_p is the attempt frequency in the potential well.⁵⁶ The fitting of our experimental data to these equations gives the attempt frequency $\omega_p = 220$ Hz and the activation energy $U_0 = 30$ K. If we assume that the transition is that from the pinned state to the sliding state, the threshold field for the transition $U_0/e\lambda_{\text{CDW}}$ estimated using the experimentally obtained U_0 becomes 1.8 kV/cm, which is in strong disagreement with the experimentally observed E_T' . And, the "pinning frequency" is too small when compared with the value obtained by the millimeter-wave technique.³⁰ These disagreements may also support the consideration that the switching is not the transition between the pinned state and the depinned state.

V. CONCLUSION

The conductivity and the time-domain current response to the dc electric field were investigated in the low-temperature switching state of $\text{K}_{0.3}\text{MoO}_3$.

By the observation of the current oscillation, this phenomenon was found to be due to the sliding motion of the CDW.

In the highly conducting state, the conductivity increases with decreasing temperature, which means that the damping by the screening of the CDW deformation by the normal carriers is almost absent in the highly conducting state. The switching was found to be well explained by the model proposed by Littlewood. The S-like I - V characteristics and the existence of the finite time delay, and the other phenomena described in the text seem to support this model.

Three types of the current response were observed in the time domain, namely the ordinary current oscillation, the relaxation-type oscillation and the quantized voltage response. Each of them is considered to correspond to the different types of the unit motion of the sliding of the CDW's. Interrelation among them was discussed. From these results, it can be said that the current oscillation is usually generated in the bulk. When the pinning at the interface becomes dominant, the amplitude mode plays an important role, as in the form of the phase-slip process or the vortex formation annihilation. Therefore, for the better description of the sliding of the CDW, the effect of the amplitude mode should be taken into account.

ACKNOWLEDGMENTS

We appreciate the helpful discussions with Dr. Hiroshi Matsukawa.

*Present address: NTT Opto-electronics Laboratories, Nippon Telegraph and Telephone Corporation, 3-1 Morinosato-wakamiya, Atsugi-shi, Kanagawa 243-01, Japan.

¹H. Fröhlich, Proc. R. Soc. London Ser. A **223**, 296 (1954).

²P. Monceau, N. P. Ong, and A. M. Portis, Phys. Rev. Lett. **37**, 602 (1976).

³For example, G. Grüner, Rev. Mod. Phys. **60**, 1129 (1988).

⁴A. Wold, W. Kunnmann, R. J. Arnott, and A. Ferretti, Inorg. Chem. **3**, 545 (1964).

⁵J. Dumas, C. Schlenker, J. Marcus, and R. Buder, Phys. Rev. Lett. **59**, 757 (1983).

⁶J. Graham and A. D. Wadsley, Acta Crystallogr. **20**, 93 (1966).

⁷J. P. Pouget, C. Noguera, A. H. Moudden, and R. Moret, J. Phys. (Paris) **46**, 1731 (1985).

⁸R. M. Fleming and L. F. Schneemeyer, Phys. Rev. B **28**, 6996 (1983).

⁹R. J. Cava, R. M. Fleming, P. Littlewood, E. A. Rietman, L. F. Schneemeyer, and R. G. Dunn, Phys. Rev. B **30**, 3228 (1984).

¹⁰R. J. Cava, R. M. Fleming, E. A. Rietman, R. G. Dunn, and L. F. Schneemeyer, Phys. Rev. Lett. **53**, 1677 (1984).

¹¹G. Kriza and G. Mihaly, Phys. Rev. Lett. **56**, 2529 (1986).

¹²A. Maeda, T. Furuyama, and S. Tanaka, Solid State Commun. **55**, 951 (1985).

¹³G. Mihaly, P. Beauchene, J. Marcus, J. Dumas, and C. Schlenker, Phys. Rev. B **37**, 1047 (1988).

¹⁴W. Folge and J. H. Perlstein, Phys. Rev. B **6**, 1402 (1972).

¹⁵L. Mihaly and G. X. Tessema, Phys. Rev. B **33**, 5858 (1986).

¹⁶A. Maeda, M. Notomi, K. Uchinokura, and S. Tanaka, Phys. Rev. B **36**, 7709 (1987).

¹⁷A. Zettl and G. Grüner, Phys. Rev. B **26**, 2298 (1982).

¹⁸L. Mihaly and G. Grüner, Solid State Commun. **50**, 807 (1984).

¹⁹K. Tsutsumi, T. Tamegai, S. Kagoshima, and M. Sato, J. Phys. Soc. Jpn. **54**, 3004 (1985).

²⁰X. J. Zhang and N. P. Ong, Phys. Rev. Lett. **55**, 2919 (1985), N. P. Ong and X. J. Zhang, Physica B+C (Amsterdam) **143B**, 3 (1986).

²¹R. M. Fleming, R. J. Cava, L. F. Schneemeyer, E. A. Rietman, and R. G. Dunn, Phys. Rev. B **33**, 5450 (1986).

²²A. Maeda, T. Furuyama, K. Uchinokura, and S. Tanaka, Physica B+C (Amsterdam) **143B**, 123 (1986).

²³L. Mihaly, K. Lee, and P. W. Stephans, Phys. Rev. B **36**, 1973 (1987).

²⁴T. Chen, L. Mihaly, and G. Grüner, Phys. Rev. Lett. **60**, 464 (1988).

²⁵G. Mihaly, P. Beauchene, T. Chen, L. Mihaly, and G. Grüner, Phys. Rev. B **37**, 6536 (1988); G. Mihaly and P. Beauchene, Solid State Commun. **63**, 911 (1987).

²⁶P. B. Littlewood, Solid State Commun. **65**, 1347 (1988).

²⁷S. Martin, R. M. Fleming, and L. F. Schneemeyer, Phys. Rev. B **38**, 3602 (1988).

²⁸G. Mihaly, T. Chen, T. W. Kim, and G. Grüner, Phys. Rev. B **38**, 3602 (1988).

²⁹J. R. Tucker and W. G. Lyons, Phys. Rev. B **38**, 7854 (1988).

³⁰G. Mihaly, T. W. Kim, and G. Grüner, Phys. Rev. B **39**, 13 009 (1989).

³¹J. Bardeen, Phys. Rev. Lett. **62**, 2985 (1989).

³²M. Notomi, A. Maeda, K. Uchinokura, and S. Tanaka, Synth. Met. **29**, F335 (1989).

³³R. M. Fleming and C. C. Grimes, Phys. Rev. Lett. **42**, 1423 (1979).

³⁴P. Monceau, J. Richard, and M. Renard, Phys. Rev. Lett. **45**, 43 (1980).

³⁵A. Maeda, T. Furuyama, K. Uchinokura, and S. Tanaka,

- Solid State Commun. **58**, 25 (1986).
- ³⁶N. P. Ong, C. B. Kalem, and J. C. Eckert, Phys. Rev. B **30**, 2902 (1984).
- ³⁷R. M. Fleming, Solid State Commun. **43**, 167 (1982).
- ³⁸M. Ido, Y. Okajima, H. Wakimoto, and M. Oda, Physica B+C (Amsterdam) **143B**, 54 (1986).
- ³⁹P. B. Littlewood, Phys. Rev. B **36**, 3108 (1987), and references cited therein.
- ⁴⁰M. L. Boriack and A. W. Overhauser, Phys. Rev. B **17**, 2395 (1978).
- ⁴¹S. Takada, K. Y. M. Wong, and T. Holstein, Phys. Rev. B **32**, 4639 (1985).
- ⁴²Y. M. Kim, G. Mihaly, and G. Grüner, Solid State Commun. **69**, 975 (1989).
- ⁴³R. P. Hall and A. Zettl, Physica B+C (Amsterdam) **143B**, 152 (1986).
- ⁴⁴L. Mihaly, T. Chen, and G. Grüner, Solid State Commun. **61**, 751 (1987).
- ⁴⁵S. H. Strogatz, C. M. Marcus, and R. M. Westervelt, Phys. Rev. Lett. **61**, 2380 (1988).
- ⁴⁶H. Fukuyama, J. Phys. Soc. Jpn. **41**, 513 (1976); H. Fukuyama and P. A. Lee, Phys. Rev. B **17**, 45 (1978).
- ⁴⁷P. A. Lee and T. M. Rice, Phys. Rev. B **19**, 3970 (1979).
- ⁴⁸A. Maeda, Ph.D. thesis, the University of Tokyo (in Japanese), 1989.
- ⁴⁹N. P. Ong and K. Maki, Phys. Rev. B **32**, 6583 (1985).
- ⁵⁰G. Grüner, A. Zawadowski, and P. M. Chaikin, Phys. Rev. Lett. **46**, 511 (1981).
- ⁵¹L. P. Gor'kov, Pis'ma Zh. Eksp. Teor. Fiz. **38**, 76 (1983) [JETP Lett. **38**, 87 (1983)]; Zh. Eksp. Teor. Fiz. **86**, 1818 (1984) [Sov. Phys.—JETP **59**, 1057 (1984)].
- ⁵²H. Matsukawa and H. Takayama, Solid State Commun. **52**, 45 (1984).
- ⁵³P. B. Littlewood, Phys. Rev. B **33**, 6694 (1986).
- ⁵⁴R. F. Voss, J. Low Temp. Phys. **42**, 151 (1981).
- ⁵⁵A. O. Calderia and A. Leggett, Phys. Rev. Lett. **46**, 211 (1981).
- ⁵⁶T. A. Fulton and L. N. Dunkleberger, Phys. Rev. B **9**, 4760 (1974).
- ⁵⁷M. Devoret, J. Martinis, and J. Clarke, Phys. Rev. Lett. **55**, 1908 (1985).
- ⁵⁸D. B. Schwartz, B. Sen, C. N. Archie, and J. E. Lukens, Phys. Rev. Lett. **55**, 1547 (1985).
- ⁵⁹For systems related to present problem, see B. A. Hubermann and J. P. Crutchfield, Phys. Rev. Lett. **43**, 1743 (1979).
- ⁶⁰P. Grassberger and I. Procaccia, Phys. Rev. Lett. **50**, 346 (1983); Physica (Amsterdam) **9D**, 189 (1983).
- ⁶¹A. Ben-Mizrachi, I. Procaccia, and P. Grassberger, Phys. Rev. **29**, 975 (1984); M. Franaszek, Phys. Lett. **105A**, 383 (1984).